Petroleum and Coal

Design, Fabrication, and Validation of a Flow Loop for CO_2 Adsorption Studies

Victor. J. Aimikhe* and Emmanuel. O. Eyankware

Department of Petroleum and Gas Engineering, University of Port Harcourt, Nigeria

Abstract

The challenge posed by CO_2 emission into the atmosphere has necessitated studies into carbon capture and storage using adsorption processes at a laboratory scale. In this regard, different experimental CO_2 flow loop setups have been designed and fabricated. However, most of these loops are complex and expensive to replicate for adsorption studies, thereby limiting the advancement of adsorption-based CO_2 capture studies. As a result, this study has designed and fabricated an experimental CO_2 flow loop based on the volumetric balance adsorption approach in line with Sievert's law. The loop was used to evaluate the adsorption capacity of activated carbon prepared from corn cobs. The adsorption experiment was performed at temperatures of 26°C, 40°C, and 70°C and pressures of 5, 10, and 15 psi, consistent with post-combustion conditions, using a retention time of 60 minutes, for each measurement. Similar adsorption experiments were performed using commercial activated carbon. On comparison, the adsorption capacities, CO_2 equilibrium data and adsorption isotherm constants, of the activated carbon from corn cobs compared favourably with those of the commercial activated carbon. These results were also found to be consistent with those of other published works that used well-established experimental CO_2 adsorption flow loops.

Keywords: *CO_2 capture; Flow loop design; Activated carbon; Validation; CO_2 adsorption isotherm.*

1. Introduction

Climate change presents a perennial problem of environmental degradation to humanity [1] occasioned by the release of harmful greenhouse gases like CO_2 into the atmosphere. This harmful effect of CO_2 on the environment has resulted in increased conversation around potential solutions to mitigate climate change and ensure the world's ecosystem's sustainability. The solutions to these environmental problems are linked to reducing carbon dioxide emissions into the atmosphere [2]. The atmospheric concentration of carbon dioxide, the primary greenhouse gas responsible for global warming [3], has increased from 220 ppm in the pre-industrial era [4] to 412 ppm in 2020 [5], due mainly to the increased use of carbon-intensive fuels [6]. There exist several different technologies that have been deployed to reduce CO_2 emissions. These include planting trees, using renewable energy sources, and increased use of clean energy technologies such as carbon capture and storage (CCS). Among these technologies, CCS presents an alternative solution to global carbon footprint reduction due to its applicability in process systems that utilize "dirty" fossil fuels for energy generation, especially as fossil fuel consumption [7] has been projected to remain significant from 2020 till 2050 [6]. Also, the competitiveness of fossil fuels in the coming years will largely depend on the advancement of CO_2 capture technologies, among other factors.

Different mechanisms exist for CCS. They are absorption, adsorption, microbial/algae, cryogenic, and membranes. Although absorption, also known as amine scrubbing, technology is the most mature and popular CCS technology [8], its drawbacks include solvent degradation, corrosion, high cost of operation, and solvent evaporation. On the other hand, adsorption technology has gained a lot of attention in the recent past due to properties like low cost of operation due to low energy of regeneration, the high adsorption capacity of CO_2 adsorbents, low cost of production of adsorbents such as activated carbon, and the associated thermal,

chemical and mechanical stability [9]. In this regard, a lot of studies have been carried out to investigate the suitability of adsorbents such as metal-organic frameworks [10], carbon nano-tubes [11], activated carbon [12], and polymers [13], etc., for CO_2 capture at post-combustion conditions. A critical component of these studies is the use of a CO_2 experimental flow loop with the capacity to measure the CO_2 adsorption capacity of these adsorbents. The adsorption capacities are usually measured in volumetric or gravimetric capacities [14] (units of measurement include mmol/g, cm^3/g and mg/g).

A typical CO_2 experimental flow loop is a reliable method to determine the amount of CO_2 molecules adsorbed by adsorbents in an adsorption column via pressure, temperature, vacuum, and combined vacuum and electric swing adsorption processes. In a CO_2 flow loop, the typical protocol used to determine adsorption capacity is observing changes in the equilibrium adsorption capacity and equilibrium loading of adsorbents in contact with adsorbate under controlled conditions [15]. These CO_2 flow loops are of different designs and configurations, including packed bed reactors [16], thermogravimetric analyzers [17], and volumetric adsorption systems [18]. Adsorption capacities are evaluated based on volumetric or mass balance approaches. Different authors have optimized these configurations to address specific needs of adsorption systems for research and development purposes based on these designs, configurations, and evaluation approaches. Most of the configurations developed contained different units such as mass flow meter, mass flow controller, gas analyzer, tube furnace, data recording unit, and mass spectrometer. Due to the complexities of these designs, it becomes costly and difficult to replicate these laboratory experimental setups for adsorption studies. Consequently, it is therefore imperative to develop simpler designs that comprise less number of components at less cost while also giving accurate results. However, some of existing experimental CO_2 flow loop designs produced by different authors would be reviewed for analysis so as to highlight the need for a simpler and cost effective configuration.

Perrier, Plantier, and Grégoire[19] designed an experimental flow loop to measure simultaneous adsorption and deformation-induced measurements of microporous adsorbents for CO_2 and CH_4 capture. The flow loop consists of a home-made manometric apparatus for adsorption measurement and digital image correlation for full-field displacement and determination of induced deformation. The details and working principles of the apparatus can be found in their work [19]

Qinghua et al. reported using an experimental CO_2 flow loop for CO_2 capture using the composite of silicic acid impregnated with amine as an adsorbent [20]. In their study, the experimental setup is based on the measurement of change in CO_2 concentration (a mass balance-based approach). The setup comprises a mass flow controller, a syringe pump, tube furnace, temperature controller, moisture removal unit, gas analyzer, and data recording unit. In this configuration, the adsorption process takes place in the quartz tube placed inside a tube furnace. The details of the adsorption process are reported in their work [20].

Thiruvenkatachari et al.[21] investigated a novel configuration of an experimental setup to measure CO_2 adsorption from a stationary system that uses honeycomb monolithic carbon fiber composite adsorbents. CO_2 adsorption, regeneration, and an intermediate preparation of adsorbents for CO_2 capture can be done simultaneously in the experimental setup. It consists of a pre-treatment stage, adsorption chambers, particulate separators, swing apparatus, and gas analyzer. This experimental setup is designed to evaluate the CO_2 adsorption capacity of adsorbents using a mass balance approach via measurement of the CO_2 concentration of effluent gas.

Yang et al. [22] investigated the use of organic copolymers for CO_2 capture at pre-combustion conditions using an experimental setup that evaluates adsorption capacity via a mass balance approach. The experimental design consists of a mass flow controller, humidifier, temperature-controlled adsorption cell, and mass spectrometer. During the adsorption process, an adsorbent of a specific mass is placed in the adsorption cell, activated with an inert gas flow at a specific degassing temperature. After that, a gas mixture of particular composition is flown into the adsorption cell under the control of the mass flow controller for the adsorption process. After the adsorption process, the effluent gas is analyzed using a mass

spectrometer to determine CO_2 concentration, which is used to determine CO_2 adsorption capacity using the mass balance method.

It is evident from the selected experimental CO_2 flow loop designs reviewed that these configurations are complex, difficult to replicate, and by extension, costly. Hence, this paper discusses a recently designed and fabricated flow loop for CO_2 adsorption studies.

2. Laboratory CO_2 flow loop design

The CO_2 experimental flow loop is designed according to Sievert's law presented by Sadie [23], with temperature and pressure ranges of 0 – 100°C and 0 – 15 psi. Figure 1 shows the experimental configuration of the adsorption loop designed and fabricated for use in this study. The setup comprises a water bath, an adsorption Reactor (R), staging manifold (SM), one horsepower (hp) vacuum pump, CO_2 storage cylinder, pressure gauges, connecting valves, and stainless steel connecting pipes. Figure 2 shows the adsorption reactors. Table 1 shows the functions of each of these components.
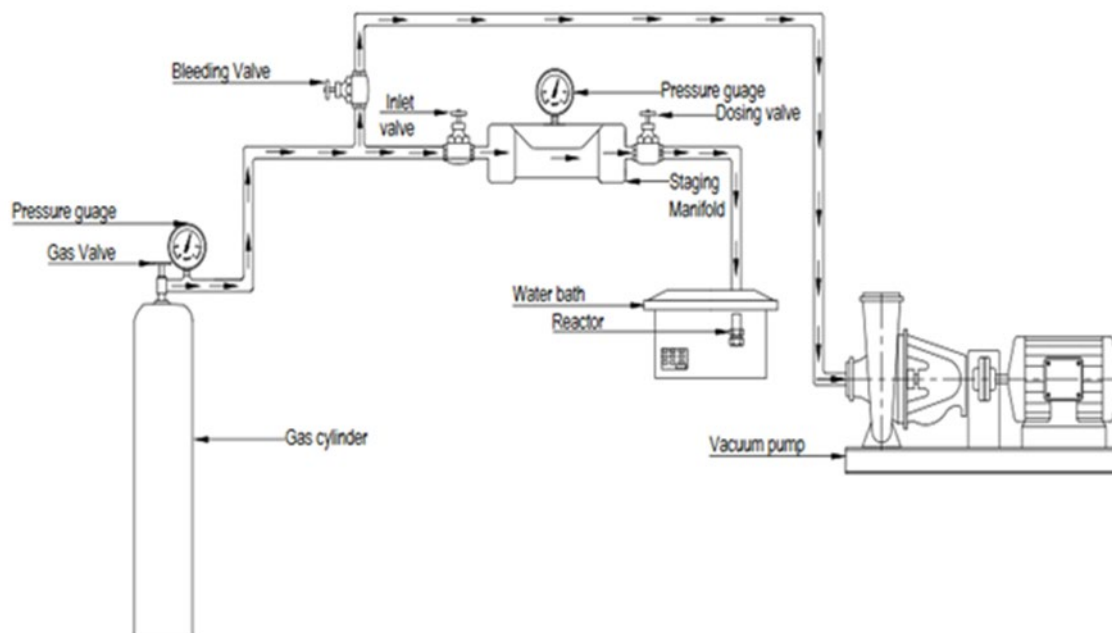

Fig. 1. Schematic of experimental setup in this study

Fig. 2. Reactors for storing adsorbents

Table 1. Function of loop components

S/N	Component	Function
1	Gas Cylinder (GC)	This unit stores the CO_2 gas at a 98% purity level.
2	Gas Valve	This unit controls the flow of CO_2 gas from the gas cylinder to the staging manifold.
3	Pressure Gauge (PG)	This unit measures the pressure of CO_2 gas inside the gas cylinder and staging manifold.
4	Bleeding valve (BV)	This unit facilitates the removal of CO_2 gas from the experimental setup.
5	Inlet valve (IV)	This unit controls the flow of CO_2 gas into and out of the staging manifold
6	Dosing valve (DV)	This unit controls the flow of CO_2 gas into and out of the reactor.
7	Staging manifold (SM)	This unit stores CO_2 gas for equilibrium conditions to be achieved.
8	Reactor (R)	This unit functions as the adsorption column that houses the adsorbent.
9	Water bath (WB)	This unit controls the temperature of the reactor.

Table 2. Section dimensions of CO_2 flow loop

S/N	Volumes	Magnitude (ft^3)
1	Volume after IV, but before DV (V_1); denoted as V_i	1.71×10^{-2}
2	Volume after DV (V_2)	7.01×10^{-4}
3	Volume of reactor ($V_{reactor}$)	3.14×10^{-4}
4	Volume occupied by adsorbent in Reactor (V_s)	1.57×10^{-4}
5	Volume available for CO_2 to occupy before adsorption (V_f)	1.76×10^{-2}
6	Volume of Apparatus before WB at isothermal regions (V_{app})	1.74×10^{-2}
7	Volume of apparatus immersed in WB at isothermal regions (V_{bath})	2.03×10^{-4}
8	Ratio of V_{bath} to V_{app} at isothermal regions (b)	2.06×10^{-2}
9	Final volume occupied by gas molecules in apparatus ($V_{f,app}$)	1.69×10^{-2}
10	Final volume occupied by gas molecules in WB ($V_{f,bath}$)	3.63×10^{-4}

2.1. Determination of CO_2 adsorption capacity of the experimental setup

The volumetric method approach is applied in determining the adsorption uptake of gas by the adsorbent. Table 2 highlights the dimensions of the CO_2 experimental setup used for calculation. V_1 was calculated using Equation 1. This volume includes the volume of the flowlines after the inlet valve (IV) and before the dosing valve (DV).

$$V_1 = (\pi r^2 h)_{\text{staging manifold}} + 3[(\pi r^2 h)_{\text{flowlines}}] \qquad (1)$$

The $3[(\pi r^2 h)_{\text{flow lines}}]$ consist of the segment of pipes between the staging manifold and the inlet valve, the pressure gauge, and the dosing valve.

where: V_1 = volume of staging manifold and flow lines (ft^3); r = internal radius of flowline (inches); h = length of flowline (inches).

Also, the volume of the system after DV was calculated using a volume of reactor and flow line after DV using Equation 2;

$$V_2 = (\pi r^2 h)_{\text{reactor}} + (\pi r^2 h)_{\text{flow line}} \qquad (2)$$

where: V_2 = Volume of reactor and flowline after DV (ft^3); Furthermore, the volume of apparatus (V_{app}) was calculated from Equation 3;

$$V_{app} = V_1 + (\pi r^2 h)_{\text{flow lines}} \qquad (3)$$

where: V_{app} = Volume of apparatus before WB (ft^3).

The volume of apparatus in the water bath (V_{bath}) was calculated using Equation 4;

$$V_{bath} = V(\pi r^2 h)_{\text{reactor}} + V(\pi r^2 h)_{\text{flowline in WB}} \qquad (4)$$

where: V_{bath} = Volume of apparatus in the water bath(ft^3); $V_{reactor}$ = Volume of Reactor (ft^3); $V_{\text{flowline in WB}}$ = Volume of flow line in WB (ft^3).

The ratio of volumes of isothermal regions, b was calculated using Equation 5;

$$b = \frac{V_{bath}}{V_{app}} \qquad (5)$$

where: b = Ratio of volumes at isothermal regions; V_{bath} = Volume of apparatus in WB(ft^3); V_{app} = Volume of apparatus before WB(ft^3).

After equilibration, the final volume of gas adsorbed in the two isothermal regions was calculated using Equations 6 and 7.

$V_{f, app} = (1 - b)V_f$ (6)

$V_{f, bath} = bV_f$ (7)

where: $V_{f, app}$ = Final volume occupied by gas molecules in apparatus(ft^3); $V_{f, bath}$ = Final volume occupied by gas molecules in WB (ft^3); b = ratio of the volume of isothermal regions; V_f = Final volume available for gas molecules to occupy(ft^3).

Furthermore, the initial number of gas molecules available for adsorption was calculated using Equation 8;

$n_i = \rho\left[P_i, T_{app}\right]V_i$ (8)

where: n_i = initial number of moles of CO_2 gas; ρ = density of gas at a particular pressure (psi) and temperature (ºF) (lb/ft^3); P_i = initial pressure of CO_2 gas (psi); T_{app} = Temperature of apparatus (ambient conditions, 26ºC).

The final number of moles (n_f) was calculated using Equation 9;

$n_f = \rho\left[P_f, T_{app}\right]V_{f,app} + \rho\left[P_f, T_{bath}\right]V_{f,bath}$ (9)

where: n_f = final number of moles of CO_2 gas; ρ = density of gas at a particular pressure (psi) and temperature (ºF) (lb/ft^3); P_f = Final pressure of CO_2 gas (psi); T_{bath} = Temperature of water bath (ºC).

The density (ρ) of CO_2 was calculated using Equation 10. Since PV = ZnRT

$PV = Z\frac{m}{M_a}RT$; $\rho = \frac{m}{v} = \frac{PM_a}{ZRT}$ (10)

where: Z = 1 at low pressures (5 – 15 psi); M_a = Molecular weight of CO_2; R = The universal gas constant (10.732 ft^3/lb-mol ºR).

Finally, the number of moles (n_e) adsorbed by adsorbents was calculated using Equation 11;

$n_e (P_f, T_{bath}) = n_i - n_f$ (11)

where: n_e = number of moles of CO_2 adsorbed by the adsorbent; n_i = initial number of moles of CO_2 gas; n_f = final number of moles of CO_2 gas.

2.2. CO₂ adsorption experimental procedure

In the process of experimentation, the reactor (R) was filled to half its volume with AS and CAC for the two different adsorption experiments. The DV was shut, IV and BV opened, and VP was carefully used to remove air molecules from the air-tight apparatus to ensure no other gases in the system before the adsorption process began. After that, 60 minutes was allowed for the temperature of the reactor and water bath to equilibrate. Then, DV and BV were shut while IV was opened for CO_2 gas to flow into SM from CG.

The pressure in V_1 was allowed to build up to a specific pressure of interest (P_1 = 2.0, 3.0, 4.0, 5.0, 6.0, 8.0, 10.0, and 15.0 psi). The inlet valve (IV) was quickly closed to maintain constant pressure in V_1 and observed for 15 minutes to check for any leakages. The dosing valve (DV) was carefully opened so that CO_2 gas can flow into V_2 immersed in a water bath (WB) at a particular temperature. A period of 60 minutes was allowed for proper adsorption to occur in V_2, and the final pressure (P_2) was read from the pressure gauge (PG) and recorded.

The experiment was repeated at the end of each sorption cycle for incremental pressures and temperatures, using a specific adsorbent. The procedure described in this section above was repeated to continue another sorption cycle using a different adsorbent.

2.3. Validation of loop

The validation of the experimental CO_2 flow loop used in this study was done using two different adsorbents at post-combustion conditions of 5 to 15 psi, at 26ºC, 40ºC, and 70ºC. The adsorbents used were activated carbon samples (AS) prepared from corn cobs, and commercial activated carbon (CAC) obtained from commercial vendors. The (AS) samples were carbonized for 30 mins and activated using potassium hydroxide (KOH) at room temperature for 72 hours. Adsorption capacities and isotherms of the AS and CAC were compared for possible similarities. The results were also compared with similarly published works of other researchers. This comparison was made to ascertain the accuracy of the developed CO_2 loop for adsorption studies.

3. Results and discussion

Figures 3 and 4 show the Langmuir and Freundlich isotherms of AS and CAC at 26°C, 40°C, and 70°C and ambient pressure. The results reveal similar trends for the adsorption isotherms. Also, the CO_2 adsorption capacity of AS outperformed CAC at all process conditions investigated. The results indicate that CO_2 adsorption capacity reduced as temperature increased from 26°C, 40°C, and 70°C at ambient pressures for both AS and CAC. This trend shows that the process of adsorption is physisorption-driven as the reduction in CO_2 adsorption capacity can be attributed to a loss in binding strength of adsorbates on the adsorbents (AS and CAC inclusive) facilitated by weak van der Waals forces. An increase in adsorption temperature increased the internal energy of the system, which led to a release of CO_2 adsorbates, indicating an exothermally driven adsorption process. These results and trends are similar to the results reported by other researchers [24-25], indicating the suitability of the experimental CO_2 flow loop developed in this study for adsorption studies.
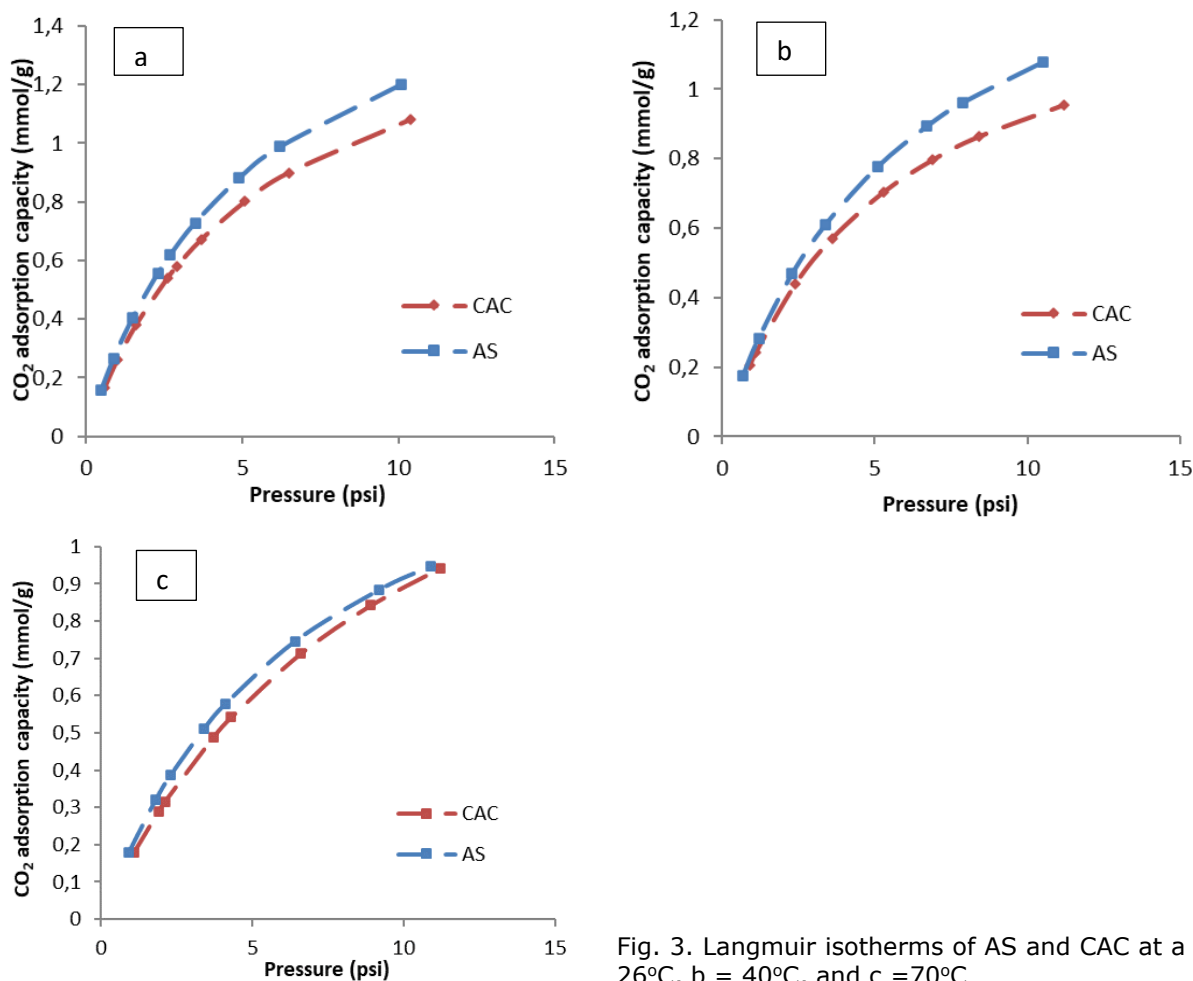

Fig. 3. Langmuir isotherms of AS and CAC at a = 26°C, b = 40°C, and c =70°C

Table 3 shows the predicted Langmuir and Freundlich adsorption isotherm constants obtained from non-linear regression models. The results for the Langmuir (K_L) and Freundlich constants (K_F) showed that an increase in the temperature of adsorption resulted in a decrease in isotherm constants, highlighting a physisorption driven process as also reported by Rashidi [26]. Furthermore, the R^2 values for the Langmuir isotherms of AS at 26°C, 40°C, and 70°C were higher than the R^2 values for the Freundlich isotherms at the same temperatures. These results reveal that adsorption on the AS using the fabricated CO_2 flow loop in this study is done on a monolayer interface. Similar results were obtained by other authors in the published literature [27].
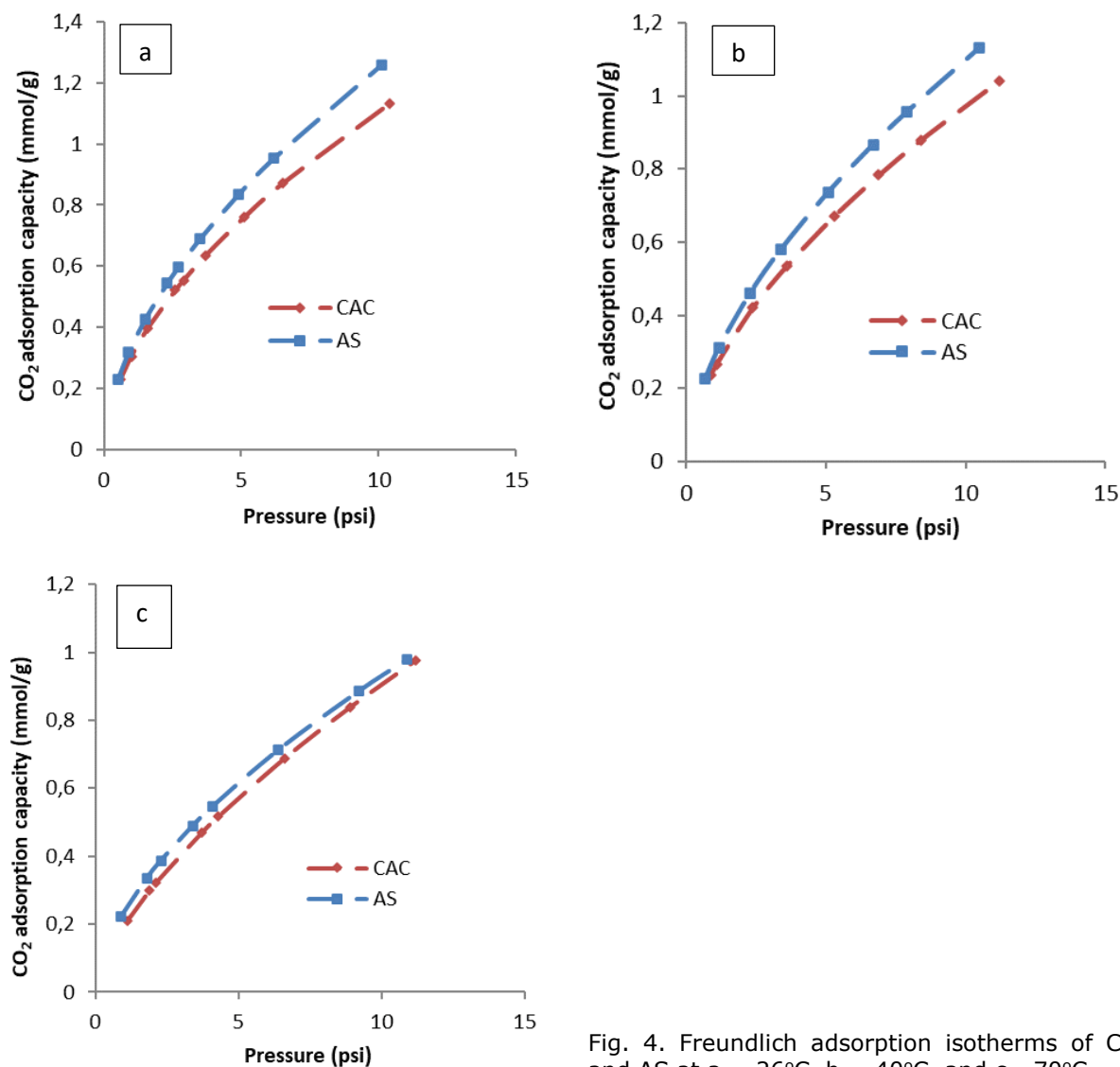
Fig. 4. Freundlich adsorption isotherms of CAC and AS at a = 26°C, b = 40°C, and c =70°C

Table 3. Parameters of Langmuir (Lang.) and Freundlich (Freun.) Isotherms at 26°C, 40°C, and 70°C

Sample		26°C		40°C		70°C	
Isotherm type		Lang.	Freun.	Lang.	Freun.	Lang.	Freun.
AS	q_m (mmol/g)	1.5977	-	1.3526	-	1.2369	-
	K_L	0.1666	-	0.1440	-	0.1256	-
	K_F	-	0.2672	-	0.2584	-	0.2321
	n	-	1.7131	-	1.7996	-	1.9839
	R^2	0.9957	0.9814	0.9875	0.9696	0.9801	0.9680
CAC	q_m (mmol/g)	1.6526	-	1.4000	-	1.2495	-
	K_L	0.1903	-	0.1514	-	0.1044	-
	K_F	-	0.3046	-	0.2505	-	0.2167
	n	-	1.7817	-	1.6945	-	1.5096
	R^2	0.9134	0.9712	0.9268	0.9826	0.9684	0.9911

On the other hand, the R^2 values of Freundlich isotherms of CAC at 26°C, 40°C, and 70°C were higher than the R^2 values of Langmuir isotherm constants, at the same temperatures. This R^2 result shows that CO_2 adsorption on the CAC adsorbent surface occurs under multilayer conditions. This result is similar to the one reported by Rashidi [26].

4. Conclusion

In this paper, an experimental CO_2 flow loop for adsorption studies has been designed, fabricated, and validated. The flow loop currently operates at temperatures of 0 – 100°C and pressures of 0 – 15 psi. The experimental setup was used to study CO_2 adsorption at post-combustion conditions using AS and CAC at temperatures of 26, 40, and 70°C and pressures of 5, 10, and 15 psi. The results showed that the developed CO_2 flow loop could adequately predict CO_2 equilibrium data and adsorption isotherms of CO_2 capture processes at post-combustion conditions.

List of symbols

V_1	Volume of Staging Manifold and flow lines (ft^3)
r	internal radius of flowline (inches)
h	length of flowline (inches)
V_2	Volume of reactor and flowline after dosing valve (ft^3)
V_{app}	Volume of apparatus before water bath (ft^3)
V_{bath}	Volume of apparatus in the water bath(ft^3)
$V_{reactor}$	Volume of Reactor (ft^3)
$V_{flowline\ in\ WB}$	Volume of flow line in water bath (ft^3)
b	Ratio of volumes at isothermal regions
$V_{f,\ app}$	Final volume occupied by gas molecules in apparatus(ft^3)
$V_{f,\ bath}$	Final volume occupied by gas molecules in water bath (ft^3)
V_f	Final volume available for gas molecules to occupy(ft^3)
n_i	initial number of moles of CO_2 gas
ρ	density of CO_2 gas at a particular pressure and temperature (lb/ft^3)
P_i	Initial pressure of CO_2 gas (psi)
T_{app}	Temperature of apparatus (ambient conditions, 26°C)
n_f	final number of moles of CO_2 gas
n_e	number of moles of CO_2 adsorbed by the adsorbent
P_f	Final pressure of CO_2 gas (psi)
T_{bath}	Temperature of water bath (^{o}C)
Z	gas compressibility factor
M_a	Apparent molecular weight of CO_2
R	The universal gas constant (10.732 ft^3/lb-mol ^{o}R)
q_m	Absorption capacity (mmol/g)
K_L	Langmuir constant
K_F	Freundlich affinity constant
n	adsorption intensity
R^2	Coefficient of determination

Disclosure statement

Conflict of Interest: The authors declare that there are no conflict of interest.

Acknowledgements

References

[1]   Ciscar J.C, Iglesias A, Feyen L, Szabó L, Van Regemorter D, Amelung B, Nicholls R, Watkiss P, Christensen O, Dankers R, Garrote L, Goodess C, Hunt A, Moreno A, Richards J, Soria A. Physical and economic consequences of climate change in Europe, Proc. Natl. Acad. Sci. U. S. A. 108, 2011; 2678–2683.

[2]   Eyankware OE, Ateke IH. Methane and Hydrogen Storage in Metal-Organic Frameworks: A Mini-Review, J. Environ. Earth Sci, 2020; 56–68.

[3] United States Environmental Protection Agency, Inventory of U.S. Greenhouse Gas Emissions and Sinks: 1990-2017, 2019.

[4] Joos F, Spahni R. Rates of change in natural and anthropogenic radiative forcing over the past 20 000 years, PNAS, 105, 2008; 1425–1430.

[5] National Oceanic and Atmospheric Administration, Monthly Average Mauna Loa CO_2, 2020. https://www.esrl.noaa.gov/gmd/ccgg/trends/.

[6] Aimikhe VJ, Eyankware OE. Adsorbents for Noxious Gas Sequestration: State of the Art, J. Sci. Res. Reports, 2019; 25: 1–21. doi:10.9734/JSRR/2019/v25i1-230176.

[7] Yang Y, Yang C, Bae T. Polyamine-appended porous organic polymers for efficient post-combustion, Chem. Eng. J, 2019; 358:1227–1234.

[8] Kim S, Shi H, Lee J. CO2 absorption mechanism in amine solvents and enhancement of CO_2 capture capability in blended amine solvent, Int. J. Greenh. Gas Control, 2016; 45: 181–188.

[9] Creamer AE, Gao B. Carbon-based adsorbents for post-combustion CO2 capture: A critical review, Environ. Sci. Technol, 2016; 50:7276–7289.

[10] Yoo DK, Khan NA, Jhung SH. Polyaniline-loaded metal-organic framework MIL-101 (Cr): Promising adsorbent for CO_2 capture with increased capacity and selectivity polyaniline introduction, J. CO_2 Util, 2018; 28:319–325.

[11] Liu Q, Shi Y, Zheng S, Ning L, Ye Q, Tao M, He Y. Amine-functionalized low-cost industrial-grade multi-walled carbon nanotubes for the capture of carbon dioxide, J. Energy Chem, 2014; 23: 111–118.

[12] Singh G, Lakhi KS, Ramadass K, Sathish CI, Vinu A. High-performance biomass-derived activated porous biocarbon for combined pre-and post-combustion CO_2 capture. ACS Sustain. Chem. Eng, 2019; 7: 7412–7420.

[13] Shao L, Li Y, Huang J, Liu YN. Synthesis of Triazine-Based Porous Organic Polymers Derived N-Enriched Porous Carbons for CO_2 Capture, Ind. Eng. Chem. Res, 2018; 57: 2856–2865.

[14] He Y, Zhou W, Qian G, Chen B. Methane storage in metal-organic frameworks, Chem. Soc. Rev, 2014; 43: 5657–5678.

[15] Grande CA. Advances in Pressure Swing Adsorption for Gas Separation, ISRN Chem. Eng, 2012; 1–13.

[16] Gebald C, Wurzbacher JA, Borgschulte A, Zimmermann T, Steinfeld A. Single-component and binary CO_2 and H_2O adsorption of amine-functionalized cellulose, Environ. Sci. Technol, 2014; 48 :2497–2504.

[17] Andreoli E, Cullum L, Barron AR. Carbon dioxide absorption by polyethyleneimine-functionalized nanocarbons: A kinetic study, Ind. Eng. Chem. Res, 2015; 54: 878–889.

[18] Didas SA, Sakwa-Novak MA, Foo GS, Sievers C, Jones CW. Effect of amine surface coverage on the Co-adsorption of CO_2 and water: Spectral deconvolution of adsorbed species, J. Phys. Chem. Lett. 2014; 5: 4194–4200.

[19] Perrier L, Plantier F, Grégoire D. A novel experimental setup for simultaneous adsorption and induced deformation measurements in microporous materials, Rev. Sci. Instrum, 2017; 88.

[20] Lai Q, Diao Z, Kong L, Adidharma H, Fan M. Amine-impregnated silicic acid composite as an efficient adsorbent for CO_2 capture, Appl. Energy, 2018; 223: 293–301.

[21] Thiruvenkatachari R, Su S, An H, Yu XX. Post-combustion CO2 capture by carbon fiber monolithic adsorbents, Prog. Energy Combust. Sci, 2009; 35:438–455.

[22] Yang Y, Chuah CY, Gong H, Bae TH. Robust microporous organic copolymers containing triphenylamine for high-pressure CO_2 capture application, J. CO_2 Util, 2017; 19: 214–220.

[23] Stadie N. Experimental Adsorption Measurements, 2013. https://thesis.library.caltech.edu/7198/77/Stadie_N_2013_Appendices.pdf.

[24] Hauchhum L, Mahanta P. Kinetic, Thermodynamic, and Regeneration Studies for CO_2 Adsorption onto Activated Carbon, Int. J. Adv. Mech. Eng, 2014; 4: 27–32.

[25] Rashidi NA, Yusup S, Hameed BH. Kinetic studies on carbon dioxide capture using lignocellulosic based activated carbon, Energy, 2013 61:440–446.

[26] Adilla N, Yusup S, Borhan A. Isotherm and Thermodynamic Analysis of Carbon Dioxide on Activated Carbon, Procedia Eng, 2016; 148: 630–637.

[27] Cen Q, Fang M, Xu J, Luo Z. Experimental study of breakthrough adsorption on activated carbon for CO_2 capture, Adv. Mater. Res 2012; 356–360.

To whom correspondence should be addressed: Dr. Victor. J. Aimikhe, Department of Petroleum and Gas Engineering, University of Port Harcourt, Nigeria, E-mail: *victor.aimikhe@uniport.edu.ng*